Environ Sci Pollut Res (2015) 22:10919–10929
DOI 10.1007/s11356-015-4276-2

RESEARCH ARTICLE

Synthesis and characterization of hydroxyapatite nanoparticles impregnated on apple pomace to enhanced adsorption of Pb(II), Cd(II), and Ni(II) ions from aqueous solution

Piar Chand · Yogesh B. Pakade

Received: 16 December 2014 / Accepted: 23 February 2015 / Published online: 15 March 2015

Abstract Hydroxyapatite nanoparticles were synthesized, characterized, and impregnated onto apple pomace surface (HANP@AP) for efficient removal of Pb(II), Cd(II), and Ni(II) ions from water. HANP@AP was characterized by Fourier transform infrared spectroscopy (FTIR), scanning electron microscopy (SEM), energy-dispersive spectroscopy (EDS), transmission electron microscope (TEM), X-ray diffraction (XRD), and surface area analysis. Batch sorption studies were carried out to investigate the influence of different parameters as amount of dose (g), pH, time (min), and initial concentration (mg L^{-1}) on adsorption process. Experimental kinetic data followed pseudo-second-order model and equilibrium data well fitted to Langmuir adsorption model with maximum adsorption capacities of 303, 250, and 100 mg g^{-1} for Pb(II), Cd(II), and Ni(II) ions, respectively. Competitive adsorption of Pb(II), Cd(II), and Ni(II) ions in presences of each other was studied to evaluate the removal efficiency of HANP@AP against multi metal-loaded water. HANP@AP was successfully applied to real industrial wastewater with 100 % removal of all three metal ions even at high concentration. HANP@AP could be recycled for four, four, and three cycles in case of Pb(II), Cd(II) and Ni(II), respectively. The study showed that HANP@AP is fast, cost effective, and environmental friendly adsorbent for removal of Pb(II), Cd(II), and Ni(II) ions from real industrial wastewater.

Keywords Hydroxyapatite nanoparticles · Biosorption · Apple pomace · Wastewater treatment · Effluents · Health hazards

Responsible editor: Philippe Garrigues

Electronic supplementary material The online version of this article (doi:10.1007/s11356-015-4276-2) contains supplementary material, which is available to authorized users.

P. Chand · Y. B. Pakade (✉)
Hill Area Tea Science Division, CSIR-Institute of Himalayan Bioresource Technology, Palampur, Himachal Pradesh 176061, India
e-mail: yogesh.pakade75@gmail.com

P. Chand
Academy of Scientific and Innovative Research (AcSIR), CSIR–Central Road Research Institute (CRRI), P.O., Delhi–Mathura Road, New Delhi 110 025, India

Introduction

Heavy metals are serious threat to the environment and public health because of their nonbiodegradability and persistent nature (Baptista-Neto et al. 2000). The toxic metals such as Pb(II), Cd(II), and Ni(II) ions are discharged to industrial effluents by batteries, alloys, pigments, paints, adhesive plastics, smelting, mining, refineries, ceramics, galvanization, power generation, and metal finishing industries (Meski et al. 2010; Pino et al. 2006; Al-Qodah 2006). The permissible limit of these metal ions, i.e., Pb(II), Cd(II), and Ni(II) in water is 0.01/0.01, 0.003/0.005, and 0.07/0.1 mg L^{-1} according to World Health Organization/Environmental Protection Agency (WHO 2011; EPA 2011). Ingestion of these metals above stipulated limits can cause serious health hazards in aquatic organism, animals, and human beings (Ozer and Pirinççi 2006). Pb(II) causes kidney and brain damage, loss of learning ability in children, blood pressure, and disruption in hemoglobin formation (Argun et al. 2007). While Cd(II) causes damage to renal system, itai-itai disease, cardiovascular, hypertension bone damage (Friberg 1985), and Ni(II) causes cancer of lungs, bones, nose dermatitis, cyanosis, etc. (Meena et al. 2005).

Conventional methods, such as chemical precipitation, ion-exchange, reverse osmosis, and electrochemical treatment, produce large volume of chemical sludge and are highly expensive (Elouear et al. 2008). Hence, researchers have focused on renewable, sustainable, cost-effective, less toxic, and easy operational techniques for removal of toxic metal ions from wastewater (Crini 2005). Adsorption is considered as an effective, efficient and economic method for decontamination of water. Large surface area and negatively charged surface favor the adsorption of heavy metals (Ma et al. 2013). In recent years, several researchers have reported the use of agricultural and industrial wastes or their chemical modification to prepare adsorbents for removal of metals from water (Chand et al. 2014; Homagai et al. 2010; Sharma and Singh 2013; Chouchene et al. 2014; Bohli et al. 2015; Bensacia et al. 2014).

Recently, nanoadsorbents are being used for the removal of metal ions from aqueous solution (Feng et al. 2010). Nanoparticles (NPs) have high potential for the tertiary wastewater treatment technology because of their small size (1–100 nm), catalytic potential, highly reactive and large surface area, ease of separation, large number of active sites, and regeneration ability (Ali 2012). Hydoxyapatite ($Ca_{10}(PO_4)_6(OH)_2$) is an ideal adsorbent because of its high sorption capacity for heavy metals, low water solubility, easy availability, low cost, and applicability under oxidizing and reducing conditions (Meski et al. 2010; Ramesh et al. 2012). Recently, Tang et al. (2013) reported removal of Cr(VI) from aqueous solution using hydroxyapatite nanoparticles (HANPs) of different Ca/P ratios. HANPs prepared by using egg shells as $CaCO_3$ source were also investigated for the removal of Pb(II) ions from water (Meski et al. 2010). However, NPs aggregate by sedimentation or gravitation forces in aqueous solution. It can be prevented either by core-shell of metal oxide or impregnation of NPs onto solid support to keep them active (Zhu et al. 2010).

In view of above facts, HANPs were synthesized and impregnated onto apple pomace (AP) for removal of Pb(II), Cd(II), and Ni(II) from aqueous solution in current study. The impregnation of HANPs onto AP is a new approach, which has not been reported earlier. The impregnated HANP@AP was characterized by Fourier transform infrared spectroscopy (FTIR), scanning electron microscope (SEM), energy-dispersive spectroscopy (EDS), transmission electron microscope (TEM), Brunauer-Emmett-Teller (BET) equation, and zeta potential analysis. The parameters affecting adsorption (dose, pH, time, and initial concentration) were evaluated for the maximum removal of heavy metal ions in batch mode. The adsorption data was further supported by applying Langmuir, Freundlich, and Temkin isotherm models. Kinetic models like pseudo-second-order and intraparticle diffusion were also applied to the adsorption data. Regeneration study was conducted to evaluate the cost-effectiveness of HANP@AP for metal removal. Another objective of the study was practical application of the adsorbent (HANP@AP) for treatment of real industrial wastewater.

Materials and methods

Chemicals and reagents

Calcium hydroxide ($Ca(OH)_2$), ammonia solution (30 %), potassium dihydrogen phosphate (KH_2PO_4), sodium hydroxide (NaOH), and hydrochloric acid (HCl) were purchased from SDFCL, India. 1-6-Hexanediamine was obtained from MD Biomedical, France. Stock solutions (1000 mg L^{-1}) of Pb(II), Cd(II), and Ni(II) ions were prepared by dissolving appropriate amounts of lead nitrate $Pb(NO_3)_2$, cadmium nitrate $Cd(NO_3)_2$, and nickel nitrate $Ni(NO_3)_2$ of analytical grade purchased from SDFCL, India. Deionized water was obtained from Millipore direct Q3 (Millipore, France). The pH of the solutions was measured on Cyberscan PC510, Eutech, Singapore.

Collection of biosorbent

Apple pomace (AP) was collected from Himachal Pradesh Horticultural Produce Marketing and Processing Corporation (HPMC), Parwanoo, Himachal Pradesh, India. AP was brought in cold condition and stored in deep freezer at −20 °C until study. It was washed with distilled water and dried first at room temperature and then at 80 °C in oven. Dried AP was ground with electric grinder and passed through sieve of 150 μm for further adsorption study.

Synthesis of hydroxyapatite nanoparticles and its impregnation onto AP surface

KH_2PO_4 (2.5 g), 2.0 g $Ca(OH)_2$, and 30 mL of deionized water were taken in a flat bottom flask, and mixed well on mechanical shaker. 1-6-Hexanediamine (8.0 g) was added to above flask and allowed to react at 70 °C for 30 min to facilitate complete dissolution. The reaction mixture was cooled at room temperature, and ammonia solution (30 %) was added dropwise to adjust pH 10 (Tang et al. 2013; Wang et al. 2007). Pretreated AP (10 g) was added to the above reaction mixture along with NaOH and allowed to react for the next 30 min at 80 °C. Resulting adsorbent was cooled at room temperature, filtered, and washed with distilled water to remove the unwanted reactants. HANP@AP was then dried at 80 °C in oven and kept in desiccator for further adsorption studies.

Characterization of HANP@AP

Functional groups on the surface of HANP@AP were characterized by using Nicolet 6700 FTIR, Thermo Scientific, USA, with spectroscopic grade of KBr in the range of 400–4000 cm^{-1}. X-ray diffraction (XRD) measurements were performed on Bruker D8 Focus, Germany, in 2θ ranges from 5° to 80°. SEM images were obtained by using HITACHI, S3400N, Japan, Tokyo. EDS analysis was carried out on Noron-7 (Thermo Scientific, USA). TEM images of the adsorbent were obtained using 220-kV FEI Technai G^2, Netherlands. Surface area of HANP@AP was obtained by N_2 adsorption using Micromeritics ASAP-2000 and calculated by BET method. Particle size and zeta potential of the adsorbent were measured by using Zetasizer Nano ZS (Malvern, UK) at 25 °C. The residual concentrations of Pb(II), Cd(II), and Ni(II) ions were estimated by atomic absorption spectrophotometer (AAS) Shimadzu 6300, Japan.

Batch sorption experiment

Batch sorption experiments were conducted in 250-mL volumetric flask with 50 mg L^{-1} of HANP@AP in 50-mL solutions of different concentrations of each metal in water at room temperature. Factor influencing the adsorption process, i.e., amount of dose (0.01–0.1 g), pH (2–8), time (5–210 min), concentration (10–300 mg L^{-1}), and temperature (293–333 K), were optimized for maximum removal of each metal ion from aqueous solution. Experiments were conducted by changes one parameter which is under study and keeping the others constant. pH of the aqueous solution was adjusted with 0.1 M of NaOH and HCl. Conical flasks were shaken on mechanical shaker to attain the equilibrium under different experimental conditions. Once equilibrium was achieved, flask contents were filtered through Whatman filter paper for determination of residual metal ions in aqueous solution. The amount of metal adsorbed onto adsorbent surface was calculated by the difference in the initial and final metal concentration. Adsorption capacity (q_e) (mg g^{-1}) and removal efficiency (E %) were calculated by applying the following equations 1 & 2 respectively.

$$q_e = \frac{C_0 - C_f}{w} \times V \quad (1)$$

$$E = \frac{C_0 - C_f}{C_0} \times 100 \quad (2)$$

where C_0 and C_f are initial and final metal ion concentrations after equilibrium (mg L), w is the amount of adsorbent (g), and V is the volume of working solution (L).

Collection of real wastewater samples

Industrial wastewater samples were collected from industrial hub of Himachal Pradesh, Baddi, district Solan, from eight different locations where the industries of paints, batteries, and pharmaceutical were found in high density. Samples were collected in 2.5 L of plastics bottles and brought to laboratory for physicochemical characterization and adsorption study.

Regeneration study

Adsorption of metal ions onto HANP@AP was conducted with 0.5 g of adsorbent in 50mL metal solution having concentration of 50 mg L^{-1}. The suspensions were then kept for 1 h with shaking at 140 rpm. The loaded metal ions Pb(II), Cd(II), and Ni(II) were then desorbed by 0.05 M HNO_3 solution with agitation. The adsorbent (HAN@AP) was then washed several times with deionized water to remove residual acid and dried. It was repeatedly used for the adsorption cycle as above until its removal efficiency decreased to less than 50 %.

Results and discussion

FTIR characterization

FTIR spectra of AP before and after impregnation of HANPs are shown in Fig. 1. The surface of AP showed 12 characteristics peaks before modification as discussed in our previous study (Chand and Pakade 2013). After impregnation of HANP onto AP, most of peaks disappeared, indicating their involvement in HANP binding. These identified functional group were carbonyl (−CO) at 1635 cm^{-1}, carbonyl groups attached to aromatic ring at 1521.9 cm^{-1}, ethers (−C–O–C–) at 1384.5 cm^{-1}, carbonyl deformation (−CO) at 1259.3 cm^{-1}, −C–O stretching at 1145.7 cm^{-1}, −C–C– bonding at 546 cm^{-1}, and free amine groups ($-NH_2$) from 463 to 416 cm^{-1}. Phenolic groups (−OH) played important role in HANP binding onto AP as shown by decrease in intensity but were not fully occupied.

After the modification, characteristic bands at 3644.4, 3403.9, 2923.0, 1417.0, 1039.7, 873.5, 602.8, and 565.3 cm^{-1} were observed. The band at 3644.4 cm^{-1} was because of –NH stretching of amide groups formed from $-NH_2$ and acid (−COOH) group on the surface. The bands at 3403.9 and 2923.3 cm^{-1} were due to –OH and –CH stretching in $-CH_2$ group. The characteristics region of phosphate ($-PO_4^{-3}$) in HANPs was observed from 1470 to 565 cm^{-1}. FTIR peak at 1417.0 cm^{-1} was due to $-PO_4^{-3}$ stretching (Meski et al. 2010). The new intense bands at 1039.7, 873.5, 602.8, and 565.3 cm^{-1} were due to $-PO_4^{-3}$ stretching and vibration, stretching of $-HPO_4^{-2}$ and $-PO_4^{-3}$ bending (Wang

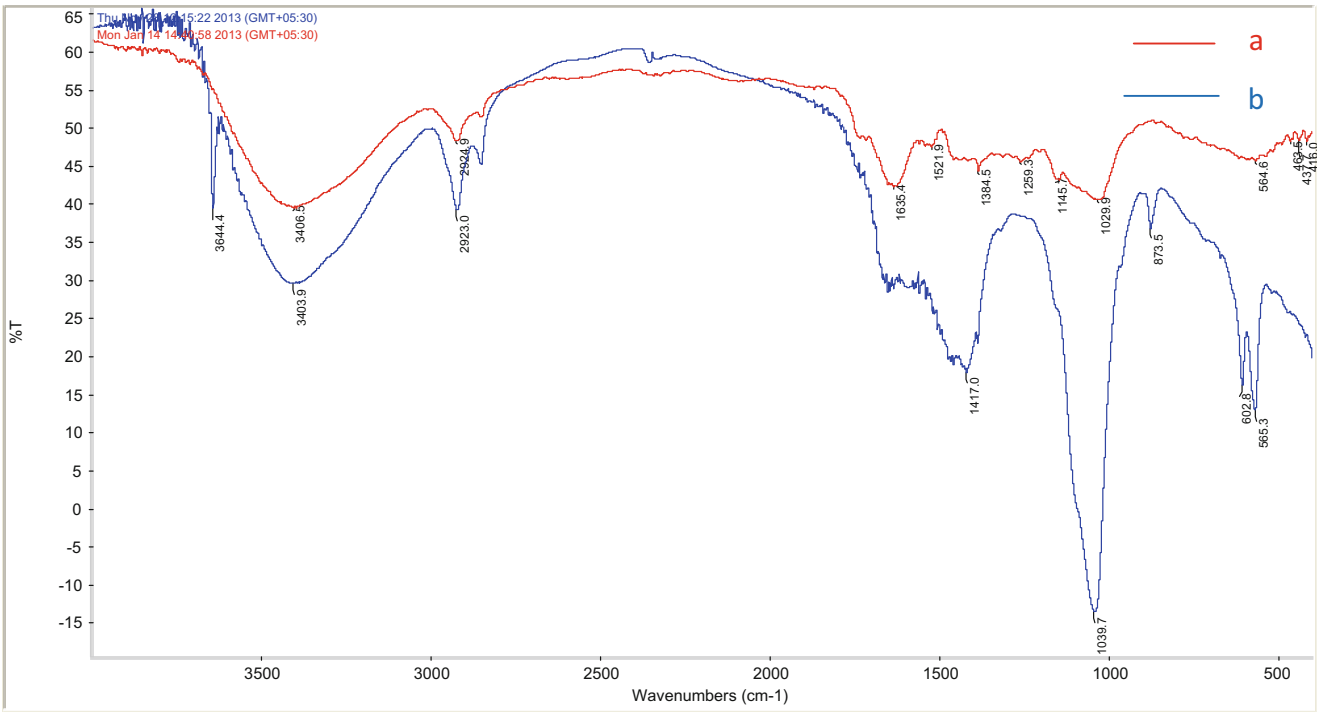

Fig. 1 Overlay of apple pomace (AP) before (**a**) and after (**b**) impregnation of HANP onto AP surface

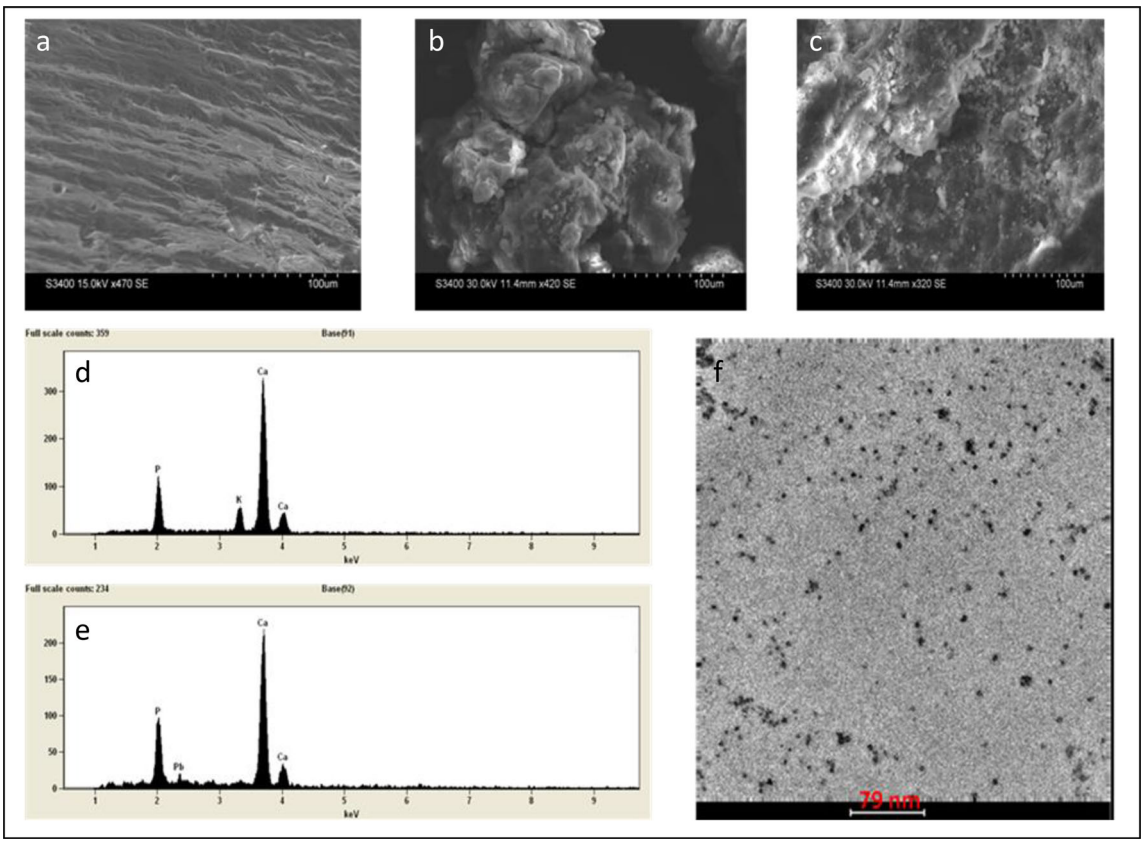

Fig. 2 Characterization of HANP@AP. SEM: **a** AP raw material before impregnation of NPs; **b** after impregnation of HANPs onto surface of AP; **c** HANPP@AP after adsorption of metal ions from aqueous solution. EDS: **d** characteristics peak of Ca, K, and P elements of NP composition were clearly shown; **e** After adsorption of Pb(II) ions, peaks are clearly shown. TEM: **f** size of NPs 79 nm and found in scattered pattern

et al. 2007). The characterized intense peaks at 1470.0, 1039.7, 873.5, 602.8, and 565.3 cm^{-1} supported the successful impregnation of HANP onto AP surface.

FTIR spectra before and after adsorption of Pb(II), Cd(II), and Ni(II) ions onto HANP@AP indicated that significant decrease in intensity of certain peaks might be involved in metal binding (Nuhoglu and Malkoc 2009). These peaks were amide (−CONH), phenols (−OH), alkene ($-CH_2$), and phosphate ($-PO_4^{-3}$) stretching at 3643.7, 3400.0, 2922.0, and 1038.8 cm^{-1} for Pb(II) while amide (−CONH), phenols (−OH), alkenes ($-CH_2$), and phosphate stretching ($-PO_4^{-3}$) at 3403.4, 2921.1, and 873.5 cm^{-1} for Cd(II) and amide (−CONH), phenols (−OH), and alkenes ($-CH_2$) for Ni(II) at 3444.4, 3428.2, and 2921.4 cm^{-1} must involved in metal adsorption onto HANP@AP surface (figures given in supporting information from Figs. 1, 2, and 3).

SEM, EDS, TEM, XRD, surface area, size, and zeta potential analyses

SEM micrographs of AP, before and after HANP impregnation, are given in Fig. 2a–c. After impregnation of HANPs, it became uneven, heterogeneous, and porous in nature. Elemental analysis of HANP@AP showed the characteristics peaks of Ca, P, and K, which were the main constituents of the adsorbent (Fig. 2d). It also demonstrated the absence of any elemental impurities, which were not used for the preparation of nanoparticles. The adsorption of metal ions Pb(II), Cd(II), and Ni(II) was confirmed by EDS analysis which were clearly observed in spectra as shown in Fig. 2e (Tseng et al. 2009). After adsorption of Pb(II), Cd(II), and Ni(II), the peaks of respective ions were clearly visible in the spectra, supporting and demonstrating the successful adsorption of metal ions onto HANP@AP surface. Surface morphology and size of HANPs were determined by TEM micrographs shown in Fig. 2f. TEM images showed that particles were in the nanoscale range with average diameter of 79 nm and spherical shape. The nanoparticles were found in scattered form and not in aggregated form, which increases the activity and availability of surface for metal ions.

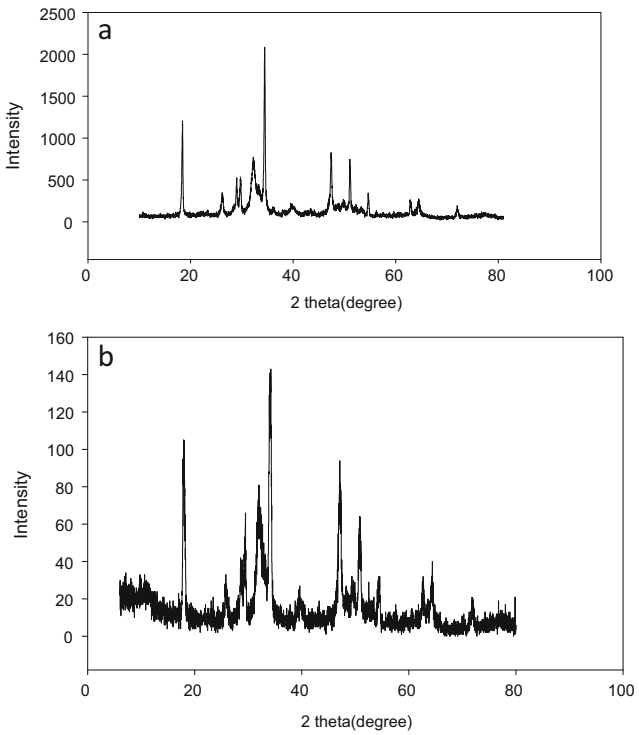

Fig. 3 XRD spectra of HANPs before (**a**) and after (**b**) impregnation onto AP surface (HANP@AP) at range of 2θ=5–80°

XRD patterns of the standard HANPs before and after impregnation onto AP surface are shown in Fig. 3a, b. Both the patterns were comparable to each other. Characteristics peaks of HANPs were clearly seen in the region of 32°–30° (2θ). According to Joint Committee on Powder Diffraction Standards (JCPDS), these peaks in between 32° and 35° (2θ) indicated the presence of pure HANP structures (Wang et al. 2007; Tseng et al. 2009; Meski et al. 2010; Tang et al. 2013). Other characteristic XRD peaks of HANPs were observed in region of 45°–55° (2θ), indicating crystalline nature of the NPs (Tang et al. 2013). After impregnation of HANPs onto the surface of AP, the characteristic peaks of HANPs were clearly observed, which demonstrated successful impregnation. However, the intensity of the peaks decreased after impregnation onto AP surface.

Surface area of the HANP@AP was found to be 52.36 $m^2\ g^{-1}$. The average particle size and zeta potential of AP were 220 d nm and −12.0 mV, respectively. After impregnation of HANPs onto AP surface, the particle size and zeta potential both increased to 826.9 d.nm and −19.7 mV, respectively. After adsorption of Pb(II), Cd(II), and Ni(II) ions onto HANP@AP, the particle size significantly increased to 1107, 1240, and 1106 d.nm, while the zeta potential decreased to −18.5, −16.19, and −17.3 mV for respective metal ions. Increase in particle size and decrease in zeta potential after adsorption of metal ions confirmed the adsorption process.

Effect of variation of adsorbent dose

The influence of adsorbent dose of HANP@AP on adsorption of Pb(II), Cd(II), and Ni(II) was studied in the range of 0.01–0.1 g, respectively. The result revealed that as the adsorbent dose increased, the adsorption of metal ions on HANP@AP also increased. As the dose increases, more surface area and new binding sites are available for metal binding (Kandah and Meunier 2007). Maximum removal levels of 99, 98, and 99 % for Pb(II), Cd(II), and Ni(II) were observed at 0.02, 0.04, and 0.06 g, respectively (Fig. 4). This is due to increase in number of binding sites for metal ions as amount of adsorbent increases. Thus, the optimum doses of HANP@AP for Pb(II),

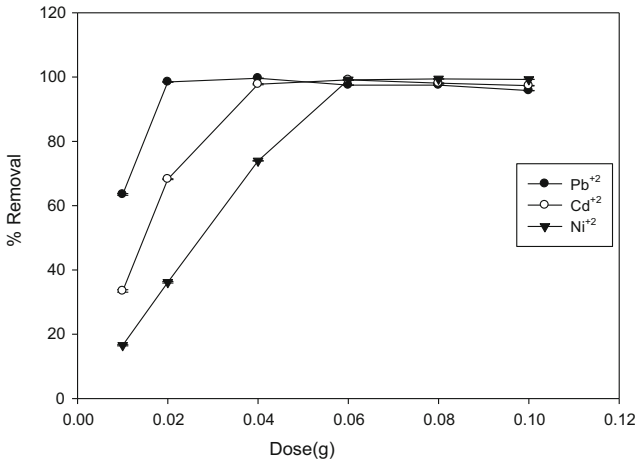

Fig. 4 Effect of adsorbent dose (0.01–0.1 g 50 mL^{-1}) for adsorption of Pb(II), Cd(II), and Ni(II) ions using HANP@AP from aqueous solution

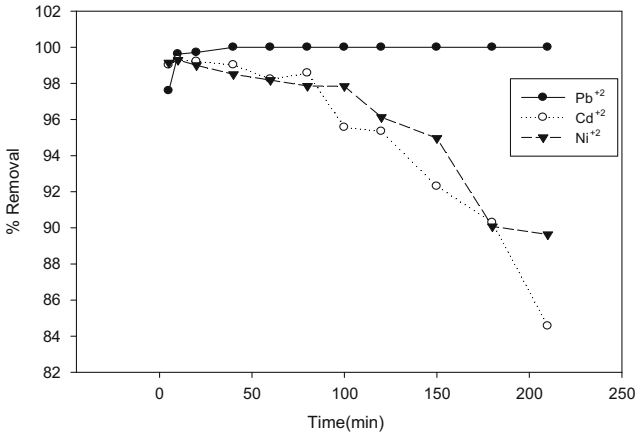

Fig. 6 Effect of time for adsorption of Pb(II), Cd(II), and Ni(II) ions from aqueous solution

Cd(II), and Ni(II) ions were found to be 0.02, 0.04, and 0.06 g, respectively.

Influence of pH, time, and initial metal ion concentration

The pH of solution has been considered as the most important variable for metal adsorption on the adsorbent. Hence, the effect of pH was investigated over the range of 2–8 as given in supporting information (Fig. 5). Optimal pH was found to be 5 with removal efficiency of 99 % for Pb(II), Cd(II), and Ni(II). At low pH, the concentration of H^+ is high, leading to competition with metal ions for vacant adsorbent sites (Feng et al. 2009). Therefore, at low pH, the adsorption efficiency was low. Increase in pH to 5 led to maximal removal of all the metal ions.

Contact time and adsorbate concentration also have pronounced effect on the adsorption process. HANP@AP could efficiently remove 98 % of all metal ions in 5 min (Fig. 6). The rapid reaction rate supported the ion exchange mechanism of metal adsorption onto surface. With further increase in time from 5 to 210 min, adsorption level did not change significantly in case of Pb(II) as the equilibrium was already established, and decreased in case of Cd(II) and Ni(II) ions. Initial metal ion concentration was varied from 10 to 300 mg L^{-1} at preoptimized adsorbent dose, pH, and time for each metal ion. The maximum concentration (100, 100, and 80 mg L^{-1}) of Pb(II), Cd(II), and Ni(II) ions was removed by less amount of HANP@AP with removal efficiency >91, >92, and >85 %, respectively. Minimum amount of dose for maximum removal of metal concentration is the requirement of advanced adsorbent treatment technology today.

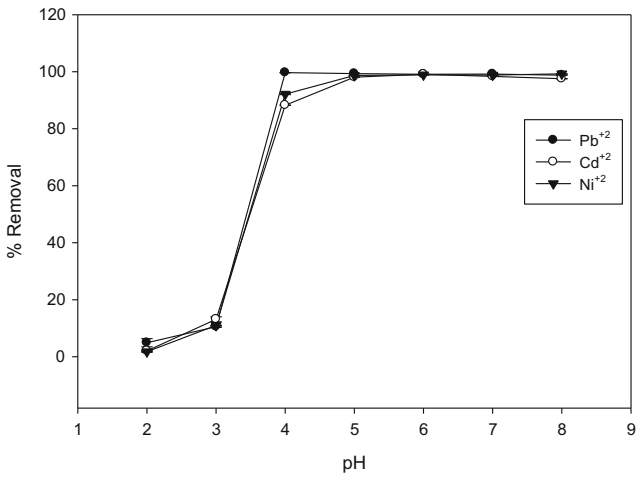

Fig. 5 Effect of pH on adsorption of Pb(II), Cd(II), and Ni(II) ions by HANP@AP from aqueous solution

Mechanism of metal binding

Mechanism of metal binding onto adsorbent surface can be described by ion exchange mechanism which involves the replacement of Ca(II) ions with M^{+2} ions, i.e., Pb(II), Cd(II), and Ni(II). It occurs in two steps. In first step, when pH was <7, the presence of the metal ions (M^{+2}) induces the dissolution of HANPs to form Ca(II), H_2PO_4, and water. It also helps to create the partial negative charges onto adsorbent surface and felicitate adsorption process (Ghasemi and Sillanpää 2015). Second step involves exchange of the Ca(II) ions with M^{+2}, i.e., Pb(II), Cd(II), and Ni(II) ions, respectively. The alkaline earth as Ca(II) metals are easily replaced by the divalent metal ions due to their labile nature by ion exchange mechanism (Cui et al. 2015; Cawthray et al. 2016). Similar mechanism was observed during the adsorption of Cu(II) ions in the presence of magnesium and sulfur onto quasi-cellulose xanthogenates products (Meski et al. 2010; Zhou et al. 2011). The most important quality of the adsorbent was the short time (<5 min) required for adsorption of 99 % of metal ions. Possible reason behind this might be the ion exchange mechanism in which Ca(II) ions were quickly replaced by the metal ions.

Adsorption isotherm

Adsorption experiments were carried out in the concentration range of 10–300 mg L^{-1} of metal ions under optimized conditions. Resulting data was applied to Langmuir, Freundlich, and Temkin isotherms (Table 1). Langmuir isotherm was found to be the most suitable with determination of coefficient (r^2) of 0.94, 0.93, and 0.96 for adsorption of Pb(II), Cd(II), and Ni(II), respectively (supplementary material). The maximum monolayer adsorption capacity of HANP@AP for Pb(II), Cd(II), and Ni(II) ions was found to be 303, 250, and 100 mg g^{-1}, respectively. Suitability of the Langmuir adsorption isotherm indicates homogenous and monolayer type of adsorption onto surface. Besides this, it assumes that all binding sites are same and bind to only one adsorbate. Also, adsorption is independent of the neighboring sites occupancy (Musico et al. 2013). The adsorption capacity (q_{max}) of HANP@AP was compared with recently reported nanoadsorbents developed by nanoparticle impregnation on supports, like chitosan beads, polystyrene, orange peel, activated carbon, zeolites, tea waste, cellulose, electrospun fibers, polystyrene CE, polystyrenesulfone-CE, polystyrene CE-D-001, and alginate (Table 2) (Liu et al. 2009; Zhang et al. 2008, 2013; Gupta and Nayak 2012; Nieto-Delgado and Rangel-Mendez 2012; Yin et al. 2012; Panneerselvam et al. 2011; Maliyekkal et al. 2010; Hota et al. 2008; Jia et al. 2009; Su et al. 2009; Ngomsik et al. 2006). The Langmuir constants for Pb(II), Cd(II), and Ni(II) ions were found to be 0.41, 0.047, and 0.248 L g^{-1}, respectively. It indicated that HANP@AP adsorption affinity followed the order Pb(II)>Ni(II)>Cd(II) ions, because the Langmuir constant is directly proportional to binding energy.

Freundlich isotherm signifies heterogeneous surface of adsorbent, but its coefficient of determination (r^2) was not satisfactory for adsorption data of metal ions. The values of Freundlich constant (K) were found to be 98.40, 23.61, and 32.99 mg g^{-1} for Pb(II), Cd (II), and Ni (II), respectively. Value of "n" for all metal ions was greater than unity, which signifies favorable adsorption of metal ions onto HANP@AP surface. Temkin isotherm assumes that liberation of heat during adsorbate-adsorbent interaction decreases linearly. Determination of coefficient (r^2) of Temkin isotherm was better than Freundlich isotherm, but not from Langmuir isotherm. Temkin constant (B) was found to be 35.62, 23.12, and 9.28 J mol^{-1} for Pb(II), Cd(II), and Ni(II) ions, respectively. The binding constant (K_t) in Temkin isotherm was 26.50, 2.96, and 80.09 for Pb(II), Cd(II), and Ni(II) ions in aqueous solution.

Kinetic study

The kinetic data was evaluated against the pseudo-second-order and intraparticle diffusion models (Ho and Mckay 2000) (data given in supplementary sheet). For kinetics study, the concentrations were varied from 10 to 80 mg L^{-1} for Pb(II), Cd(II), and Ni(II), and time was varied from 2 to 40 min for Pb(II) and Cd(II) and 2–60 min for Ni(II) ions, respectively, (Table 3). Pseudo-second-order kinetics was found to be more suitable than intraparticle diffusion model with coefficient of correlation (r^2) of 0.99–1, respectively. Intraparticle diffusion equation showed r^2 from 0.85 to 0.39 for Pb(II), 0.85 to 0.21 for Cd(II), and 0.86 to 0.26 for Ni(II) ion adsorption from aqueous solution. Intraparticle diffusion signifies that adsorption of some of the metal ions onto HANP@AP surface takes place by pore diffusion. Kinetic study revealed that equilibrium was established within 10–40 min for Pb(II) and Cd(II) and 10–60 min for Ni(II) ions, respectively.

Thermodynamic study

Temperature plays important role in adsorption process by creating new binding site through rupturing of existing bonds and increasing the mobility of metal cations. It determines the spontaneity of adsorption process. During the thermodynamic study, it was observed that adsorption of Pb(II), Cd(II), and Ni(II) ions increased with increase in temperature. Thus, the adsorption process was temperature-dependent in nature. As the temperature increased from 293 to 333 K, the negative value of change in Gibbs free energy (ΔG°) also increased, indicating the feasibility and spontaneity of adsorption of metal ions (Belala et al. 2011). At high temperatures 323 and 333 K, 100 % adsorption of Pb(II) was observed, which reduced the distribution constant (K_d) and ΔG° to zero (Table 4). The values of change in enthalpy (ΔH°) and change in entropy (ΔS°) for Pb(II) ions were positive (35.48 kJ mol^{-1} and

Table 1 Langmuir, Freundlich, and Temkin isotherms for removal of Pb(II), Cd(II), and Ni(II) ions using HANP@AP from aqueous solution

Metals	Langmuir				Freundlich				Temkin			
	Equation	q_{max} (mg g^{-1})	b (L g^{-1})	r^2	Equation	n	K_t	r^2	Equation	B	K_t	r^2
Pb(II)	y=0.008x+0.0033	303	0.41	0.94	y=0.2223x+1.993	4.49	98.40	0.76	y=35.624x+116.76	35.62	26.50	0.81
Cd(II)	y=0.0884x+0.004	250	0.047	0.93	y=0.3886x+1.3732	2.57	23.61	0.66	y=23.126x+25.083	23.12	2.96	0.82
Ni(II)	y=0.0403x+0.01	100	0.248	0.96	y=0.1921x+1.5184	5.21	32.99	0.49	y=9.2844x+40.684	9.28	80.09	0.44

Tables 2 Comparison of HANP@AP with other adsorbent impregnated with different nanoparticles for removal of Pb(II), Cd(II), and Ni(II) ions from aqueous solution

Support	NP	Metal	Adsorption capacity (mg g^{-1})	Reference
Chitosan beads	Fe^0	Pb(II), Cd(II)	55.8, 82.6	Liu et al. (2009)
Polystyrene	ZrO_2	Pb(II)	–	Zhang et al. (2013)
Orange peel	Fe_2O_3	Cd(II)	71.43	Gupta and Nayak (2012)
Activated carbon	$Fe(OH_2)_6^{+3}$	As(V)	4.56	Nieto-Delgado and Rangel-Mendez (2012)
Zeolites	Fe_2O_3	Hg(II)	–	Yin et al. (2012)
Tea waste	Fe_3O_4	Ni(II)	38.3	Panneerselvam et al. (2011)
Cellulose	β-MnO_2	Pb(II)	80.1	Maliyekkal et al. (2010)
Electrospun fiber	Boe-(AlOOH)	Cd(II)	0.20	Hota et al. (2008)
Polystyrene-CE	$Zr(HPO_3S)_2$	Pb(II), Cd(II)	–	Zhang et al. (2008)
Polystyrenesulfone-CE	$Ti(PO_4)_2$	Pb(II)	1.64	Jia et al. (2009)
polystyrene CE-D-001	Hy-MnO_2	Pb(II)	395	Su et al. (2009)
Alginate (Cyanex 272)	γ-Fe_2O_3	Ni(II)	24.65	Ngomsik et al. (2006)
Apple pomace	$(Ca_{10}(PO_4)_6(OH)_2)$	Pb(II), Cd(II), Ni(II)	303, 250, and 100	Present study

162.6 J mol^{-1} K^{-1}), indicating the endothermic nature of adsorption and increase in randomness during adsorption at junction of solid/solution interface (Ngah and Fatinathan 2008).

In case of Cd(II) and Ni(II) ions trend in value of ΔG°, ΔH°, and ΔS° was same as Pb(II) ions. ΔG° values for Cd(II) ions were found to be −3171.9, −4344.9, −4811.5, −5186.5, and −5636.8 J mol^{-1} at temperature of 293, 303, 313, 323, and 333 K, amount of dose of 0.5 g, and metal concentration of 50 mg L^{-1} of each ions, respectively. ΔH° and ΔS° values were found to be 17.12 kJ mol^{-1} and 69.9 J mol^{-1} K^{-1}, respectively. For Ni(II) ions, ΔG° values at temperatures from 293, 303, 313, and 323 K were found to be −9063.6, −9677.7, −10261.9, and −10728.3 J mol^{-1}, respectively. While at 333 K, Ni(II) adsorption was 100 %, and hence, distribution constant (K_d) was zero. K_d value of zero for Pb(II) and Ni(II) ions was because of the high binding affinity of these metals toward HANP@AP, as predicted from Langmuir isotherm. ΔH° and ΔS° for Ni(II) ions were found to be 7.31 kJ mol^{-1} and 55.9 J mol^{-1} K^{-1}, indicating the endothermic nature and increase in randomness at solid/solution interface during adsorption.

Regeneration study

Regeneration ability can make the adsorbent cost-effective, easily available, and environmental friendly. Desorption of metal-ion-loaded adsorbent was done with different acids (H_2SO_4, HCl, and HNO_3) at different molar concentrations (0.2, 0.1, and 0.05 M). Among these, the concentration of 0.05 N HNO_3 was found optimum with the maximum desorption capacity. During adsorption of Pb(II) ions, HANP@AP could be used up to three cycles with removal efficiency >98 %. The removal efficiency was >80.9 % up to five cycles, and thereafter, it decreased to <50 % (Fig. 7). In case of Cd(II) ions, >97.6 % removal was recorded up to four cycles, which decreased to 67.07 % in the fifth cycle. Similarly, the removal efficiency was <50 % after the fifth cycle in case of Ni(II) adsorption. HANP@AP could be reused up to four, four, and three cycles with removal efficiency >90 % for Pb(II),

Table 3 Pseudo-second-order of kinetics study of HANP@AP for adsorption of Pb(II), Cd(II), and Ni(II) ions from aqueous solution

Conc (mg L^{-1})	Pb(II)				Cd(II)				Ni(II)			
	Equation	r^2	K_2	$q_{e(exp)}$	Equation	r^2	K_2	$q_{e(exp)}$	Equation	r^2	K_2	$q_{e(exp)}$
10	$y=0.0227x+0.0156$	0.99	0.033	44.05	$y=0.0551x+0.0691$	0.99	0.044	18.18	$y=0.0749x+0.0059$	0.99	0.95	13.35
20	$y=0.012x+0.0012$	1	0.12	83.33	$y=0.0466x+0.0058$	0.99	0.374	21.45	$y=0.0414x+0.0028$	1	0.79	21.15
30	$y=0.0087x+0.0008$	1	0.056	149.94	$y=0.0296x+0.0104$	0.99	0.084	33.78	$y=0.0342x+0.0034$	1	0.34	29.23
40	$y=0.0064x+0.0004$	1	0.102	156.25	$y=0.0208x+0.002$	0.99	0.217	48.08	$y=0.0308x+0.0004$	1	2.10	34.46
60	$y=0.0053x+0.0017$	0.99	0.017	188.69	$y=0.0141x+0.009$	1	0.022	70.92	$y=0.0237x+0.0004$	1	1.41	42.19
80	$y=0.005x+0.0039$	0.99	0.007	200.0	$y=0.0117x+0.0011$	0.99	0.125	85.47	$y=0.0198x+0.0015$	1	0.26	50.51

Table 4 Thermodynamics study for the adsorption of the Pb(II), Cd(II), and Ni(II) ions onto HANP@AP from aqueous solution

Metals	T (K)	ΔG° (J mol^{-1})	Equation	r^2	ΔH° (kJ mol^{-1})	ΔS° (J mol^{-1} K^{-1})
Pb(II)	293	−12051.2	y=−4267.1x+19.56	0.97	35.48	162.6
	303	−14020.9				
	313	−15287.4				
	323	0				
	333	0				
Cd(II)	293	−3171.9	y=−2058.7x+8.40	0.94	17.12	69.9
	303	−4344.9				
	313	−4811.5				
	323	−5186.5				
	333	−5636.8				
Ni(II)	293	−9063.6	y=−878.81x+6.73	0.98	7.31	55.9
	303	−9677.7				
	313	−10261.9				
	323	−10728.2				
	333	0				

Cd (II), and Ni(II) ions, respectively. Regeneration of the HANP@AP makes it cost-effective and environmental friendly.

Competitive adsorption of Pb (II), Cd (II), and Ni (II) in wastewater samples

The aim of competitive adsorption study was to observe the influence of one metal ion on another during the treatment of real industrial multimetal wastewater. In multimetal system, metal ions compete with each other for the same binding sites (Hawari and Mulligan 2007). In the multimetal solutions used in this study, Pb(II)+Cd(II), Pb(II)+Ni(II), and Cd(II)+Ni(II), the adsorption of Ni(II) ions was largely affected in the presence of Pb(II) and Cd(II), while Cd(II) was less affected by the presence of Pb(II) and Ni(II) ions, and no effect was observed on Pb(II) ions in presence of Cd(II) and Ni(II). This can be explained by three possible reasons. One is the binding strength of metal ions toward binding sites, as already proposed for lead adsorption in the presence of copper, nickel, and cadmium ions (Ngah and Fatinathan 2008). Second is the density of metal ions and third one is the ionic radii, which have earlier been shown to affect biosorption of nickel and cadmium ions from industrial wastewater (Ansari and Malik 2007). The binding capacity for Pb(II) ions was found to be much higher than Cd(II) and Ni(II) ions, as calculated by Langmuir isotherm (Table 1). Once bound, no other metal ions can replace Pb(II) due to its high density.

Application of HANP@AP to real wastewater treatment

Results stemmed from our previous optimization by batch mode were applied for the treatment of real industrial wastewater using HANP@AP as adsorbent. Wastewater samples were mainly collected from eight locations of paint, battery, and pharmaceutical industries of Himachal Pradesh.

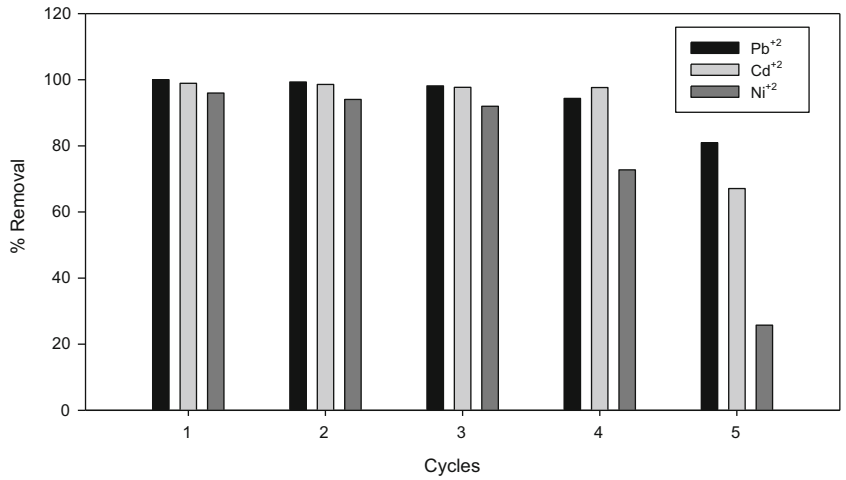

Fig. 7 Regeneration study of HANP@AP for adsorption of Pb(II), Cd(II), and Ni(II) ions

Wastewater samples were characterized for pH, total suspended solid (TSS), total dissolve solid (TDS), and metal concentration of Pb(II), Cd(II), and Ni(II) ions, respectively. pH of the samples was in the range of 5.2–7.7. TDS were found in high concentration (333.3–133.3 mg $(100\ mL)^{-1}$) than TSS of wastewater samples which were in the range of 3.0–10.3 mg $(100\ mL)^{-1}$, respectively. Metal concentrations in eight samples were found in range of 3.17–9.53 mg L^{-1} for Pb(II), 0.05–0.97 mg L^{-1} for Cd(II), and 0.17–4.78 mg L^{-1} for Ni(II) ions, respectively. HANP@AP was successfully applied to the wastewater under optimized conditions, and 100 % removal of all metal ions was observed. In order to investigate the potential of adsorbent at high metal concentration, wastewater samples were fortified with known concentration, i.e., 50 mg L^{-1} of Pb(II), Cd(II), and Ni(II) ions. At this concentration (50 mg L^{-1}), the HANP@AP was observed to 100 % removal of each metal ion from wastewater. The removal of HANP@AP was further investigated at 100 mg L^{-1} of Pb(II), Cd (II), and Ni (II) ion concentration in wastewater samples and found efficient for removal of 92.8 % for Pb(II), 100 % for Cd(II), and 68.9 % for Ni(II) ions, respectively. It shows that HANP@AP can be used as adsorbent even at high concentration (>100 mg L^{-1}) of metal ions in industrial wastewater.

Conclusions

Potential of hydroxyapatite nanoparticle impregnated on apple pomace (HANP@AP) for removal of Pb(II), Cd(II), and Ni(II) has been investigated. NPs were made of calcium, potassium, and phosphorus ions which are environmentally friendly and nontoxic. Adsorption kinetics data followed pseudo-second-order model, and adsorption isotherm was best described by Langmuir model. The maximum adsorption capacity for Pb(II), Cd(II), and Ni(II) was found to be 303, 250, and 100 mg g^{-1}, which is much higher than the existing biosorbents. The high adsorption capacity and regeneration ability of HANP@AP for removal of Pb(II), Cd(II), and Ni(II) from water make it a cost-effective adsorbent. HANP@AP was also investigated for removal of metal ions Pb(II), Cd(II), and Ni(II) to real industrial wastewater even at high concentration as potential adsorbent.

Acknowledgments The authors are thankful to the Director, Dr. P. S. Ahuja, CSIR-Institute of Himalayan Bioresource Technology, Palampur, India, for providing required research facilities. Authors are thankful to DST for providing financial support for this work. Mr. Piar Chand thankfully acknowledges the Council of Scientific and Industrial Research (CSIR), India, for providing Senior Research Fellowship (SRF) with acknowledgement number 131338/2 k11/1. Authors also acknowledge Ms. Avnesh Kumari for the help in SEM, FTIR, and EDS analyses.

Conflict of interest Authors declared that they have no conflict of interest.

References

Ali I (2012) New generation adsorbent for water treatment. Chem Rev 112:5073–5091

Al-Qodah Z (2006) Biosorption of heavy metal ions from aqueous solutions by activated sludge. Desalination 196:164–176

Ansari MI, Malik A (2007) Biosorption of nickel and cadmium by metal resistant bacterial isolates from agricultural soil irrigated with industrial wastewater. Bioresour Technol 98:3149–3153

Argun ME, Dursun S, Ozdemir C, Karatas M (2007) Heavy metal adsorption by modified oak sawdust: Thermodynamics and kinetics. J Hazard Mater 141:77–85

Baptista-Neto JA, Smith BJ, McAllister JJ (2000) Heavy metal concentrations in surface sediments in a near shore environment, Jurujuba Sound, Southern Brazil. Environ Poll 109:1–9

Belala Z, Jeguirim M, Belhachemi M (2011) Biosorption of copper from aqueous solution by date stones and palm-trees waste. Environ Chem Lett 9:65–69

Bensacia N, Fechete I, Moulay S, Hulea O, Boos A, Garin F (2014) Kinetic and equilibrium studies of lead(II) adsorption from aqueous media by KIT-6 mesoporous silica functionalized with -COOH. Comptes Rendus Chimie 17(7–8):869–880

Bohli T, Ouederni A, Fiol N, Villaescusa I (2015) Evaluation of an activated carbon from olive stones used as an adsorbent for heavy metal removal from aqueous phases. Comptes Rendus Chimie 18(1):88–99

Cawthray JF, Creagh AL, Haynes CA, Orvig C (2016) Ion exchange in hydroxyapatite with lanthanides. Inorg Chem. doi:10.1021/ic502425e

Chand P, Pakade YB (2013) Removal of Pb(II) from water by adsorption on apple pomace: equilibrium, kinetics, and thermodynamics studies. J Chem 1–8. doi:10.1155/2013/164575

Chand P, Shil AK, Sharma M, Pakade YB (2014) Improved adsorption of Cd^{2+} ions from aqueous solution using chemically modified apple pomace: mechanism kinetics and thermodynamics study. Inter Biodeter Biodegr 90:8–16

Chouchene A, Jeguirim M, Trouvé G (2014) Biosorption performance, combustion behavior, and leaching characteristics of olive solid waste during the removal of copper and nickel from aqueous solutions. Clean Technol Environmen Pol 16(5):979–986

Crini G (2005) Recent development in polysaccharide-based material used as adsorbent in wastewater treatment. Prog Polym Sci 30:38–70

Cui L, Yaoguang W, Hu L, Gao L, Du B, Wei Q (2015) Mechanism of Pb(II) and methylene blue adsorption onto magnetic carbonate hydroxyapatite/graphene oxide. RSC Adv 5:9759–9770

Elouear Z, Bouzid J, Boujelben N, Feki M, Jamoussi F, Montiel A (2008) Heavy metal removal from aqueous solution by activated phosphate rock. J Hazard Mater 156:412–420

EPA (2011) Edition of the Drinking Water Standards and Health Advisories. http://water.epa.gov/action/advisories/drinking/upload/dwstandards2012.pdf

Feng N, Guo X, Liang S (2009) Adsorption study of copper (II) by chemically modified orange peel. J Hazard Mater 164(2–3):1286–1292

Feng Y, Gong J, Zeng G, Niu Q, Zhang H, Niu C, Deng J, Yan M (2010) Adsorption of Cd(II) and Zn(II) from aqueous solution using magnetite hydroxyapatite nanoparticles as adsorbent. Chemi Eng J 162:487–494

Friberg LI (1985) Rationale of biological monitoring of chemicals—with special reference to metals. Amer Ind Hygie Ass J 46(11):633–642

Ghasemi E, Sillanpää M (2015) Magnetic hydroxyapatite nanoparticles: an efficient adsorbent for the separation and removal of nitrate and nitrite ions from environmental samples. J Sep Sci 38:164–169

Gupta VK, Nayak A (2012) Cadmium removal and recovery from aqueous solutions by novel adsorbents prepared from orange peel and Fe2O3 nanoparticles. Chemi Eng J 180:81–90

Hawari AH, Mulligan CN (2007) Effect of the presence of lead on the biosorption of copper, cadmium and nickel by anaerobic biomass. Process Biochem 42:1546–1552

Ho YS, McKay G (2000) The kinetics of sorption of divalent metal ions onto sphagnum moss peat. Water Res 34:735–742

Homagai PL, Ghimire KN, Inoue K (2010) Adsorption behaviour of toxic metals onto chemically modified sugarcane bagasse. Bioresour Technol 101:2067–2069

Hota G, Kumar BR, Ng WJ, Ramakrishna S (2008) Fabrication and characterization of a boehmite nanoparticle impregnated electrospun fiber membrane for removal of metal ions. J Mater Sci 43:212–217

Jia K, Pan B, Lv L, Zhang Q, Wang X, Pan B, Zhang W (2009) Impregnating titanium phosphate nanoparticles onto a porous cations exchanger for enhanced lead removal from waters. J Coll Interf Sci 331:453–457

Kandah MI, Meunier JL (2007) Removal of nickel ions from water by multi-walled carbon nanotubes. J Hazard Mater 146:283–288

Liu X, Hu Q, Fang Z, Zhang X, Zhang B (2009) Magnetic chitosan nanocomposites: a useful recyclable tool for heavy metal ion removal. Langmuir 25:3–8

Ma Z, Zhao D, Chang Y, Xing S, Wu Y, Gao Y (2013) Synthesis of $MnFe_2O_4$@Mn-CO oxide core-shell nanoparticles and their excellent performance for heavy metal removal. Dalton Transact. doi:10.1039/c3dt51310f

Maliyekkal SM, Lisha KP, Pradeep T (2010) A novel cellulose–manganese oxide hybrid material by in situ soft chemical synthesis and its application for the removal of Pb(II) from water. J Hazard Mater 181:986–995

Meena AK, Mishra GK, Rai PK, Rajagopal C, Nagar PN (2005) Removal of heavy metal ions from aqueous solutions using carbon aerogel as an adsorbent. J Hazard Mater 122:161–170

Meski S, Ziani S, Khireddine H (2010) Removal of lead ions by hydroxyapatite prepared from the egg shell. J Chem Eng Data 55:3923–3928

Musico YLF, Santos CM, Dalida MLP (2013) Improved removal of lead(II) from waste using a polymer assisted-based graphene oxide nanocomposites. J Mater Chem A 1:3789–3796

Ngah WSW, Fatinathan S (2008) Adsorption of Cu (II) ions in aqueous solution using chitosan beads, chitosan-GLA beads and chitosan-alginate beads. Chem Eng J 143:62–72

Ngomsik A, Bee A, Siaugue J, Cabuil V, Cote G (2006) Nickel adsorption by magnetic alginate microcapsules containing an extractant. Water Res 40:1854–1856

Nieto-Delgado C, Rangel-Mendez JR (2012) Anchorage of iron hydro (oxide) nanoparticles onto activated carbon to remove As(V) from water. Water Res 46(9):2973–2982

Nuhoglu Y, Malkoc E (2009) Thermodynamic and kinetic study of environmental friendly Ni(II) biosorption using waste pomace of olive oil factory. Bioresour Technol 100:2375–2380

Ozer A, Pirinççi HB (2006) The adsorption of Cd (II) ions on sulphuric acid treated wheat bran. J Hazard Mater 137:849–855

Panneerselvam P, Morad N, Tan KA (2011) Magnetic nanoparticles (Fe_3O_4) impregnated onto tea waste for removal of nickel (II) from aqueous solution. J Hazard Mater 186:160–168

Pino GH, Souza de Mesquita LM, Torem ML, Pinto GS (2006) Biosorption of cadmium by green coconut shell powder. Miner Eng 19:380–387

Ramesh ST, Rameshbabu N, Gandhimathi R, Nidheesh PV, Kumar MS (2012) Kinetics and equilibrium studies for the removal of heavy metals in both single and binary system using hydroxyapatite. Appl Water Sci 2:187–197

Sharma R, Singh B (2013) Removal of Ni(II) ions from aqueous solution using modified rice straw in fixed bed column. Bioresour Technol 146:519–524

Su Q, Pan B, Pan B, Zhang Q, Zhang W, Lv L, Wang X, Wu J, Zhang Q (2009) Fabrication of polymer-supported nanosized hydrous manganese dioxide (HMO) for enhanced lead removal from waters. Sci Total Environ 407:5471–5477

Tang W, Zeng R, Feng Y, Li X, Zhen W (2013) Removal of Cr(VI) from aqueous solution by nano carbonate hydroxyapatite of different Ca/P molar ratios. Chem Eng J 223:340–346

Tseng Y, Kuo C, Li Y, Huang C (2009) Polymer assisted synthesis of hydroxyapatite nanoparticles. Mater Sci Eng 29:819–822

Wang A, Liu D, Yin H, Wu H, Wada Y, Ren M, Jiang T, Cheng X, Xu Y (2007) Size controlled synthesis of hydroxide nanorods by chemical precipitation in the presence of organic modifiers. Mater Sci Eng C C27:865–869

WHO (2011) Guidelines for Drinking-water Quality fourth edition. http://whqlibdoc.who.int/publications/2011/9789241548151_eng.pdf

Yin M, Li Z, Liu Z, Yang X, Ren J (2012) Magnetic self-assembled zeolite clusters for sensitive detection and rapid removal of mercury (II). ACS Appl Mater Interf 4:431–437

Zhang Q, Pan B, Pan B, Zhang W, Jia K, Zhang Q (2008) Selective sorption of lead, cadmium and zinc ions by a polymeric cation exchanger containing nano-$Zr(HPO_3S)_2$. Environ Sci Technol 42:4140–4145

Zhang Q, Du Q, Hua M, Jiao T, Gao F, Pan B (2013) Sorption enhancement of lead Ions from water by surface charged polystyrene-supported nano-zirconium oxide composites. Environ Sci Technol 47:6536–6544

Zhou W, Ge X, Zhu D, Langdon A, Deng L, Hua Y, Zhao J (2011) Metal adsorption by quasi cellulose xanthogenates derived from aquatic and terrestrial plant materials. Bioresour Technol 102:3629–3631

Zhu Y, Stubbs LP, Ho F, Liu R, Ship CP, Maguire JA, Hosmane NS (2010) Magnetic nanocomposites: a new perspective in catalysis. Chem Cat Chem 2:365–374